Chapter 1

Experiment

1.1 Discharge Apparatus

The design of the RPND apparatus was similar to the coaxial geometry used by Vasilyak and others in FIW studies [1]. Broadly, it was comprised of cylindrical inner conductor, surrounded by a dielectric, surrounded by an outer conductor. In this case, two electrodes and the RPND between them served as the inner conductor. The dielectric was provided by a glass tube and an air gap. Finally, the outer conductor was an aluminum shell. This configuration has the benefit of minimizing the undesired inductance of the system which could inhibit the propagation of the exciting voltage pulse. The geometry and its electrical equivalent are sketched in figure 1.1. Following from right to left, the inner conductor was composed of a vacuum window, a Conflat nipple, a double-sided flange tapped for an NPT connection, and the discharge tube containing the plasma.

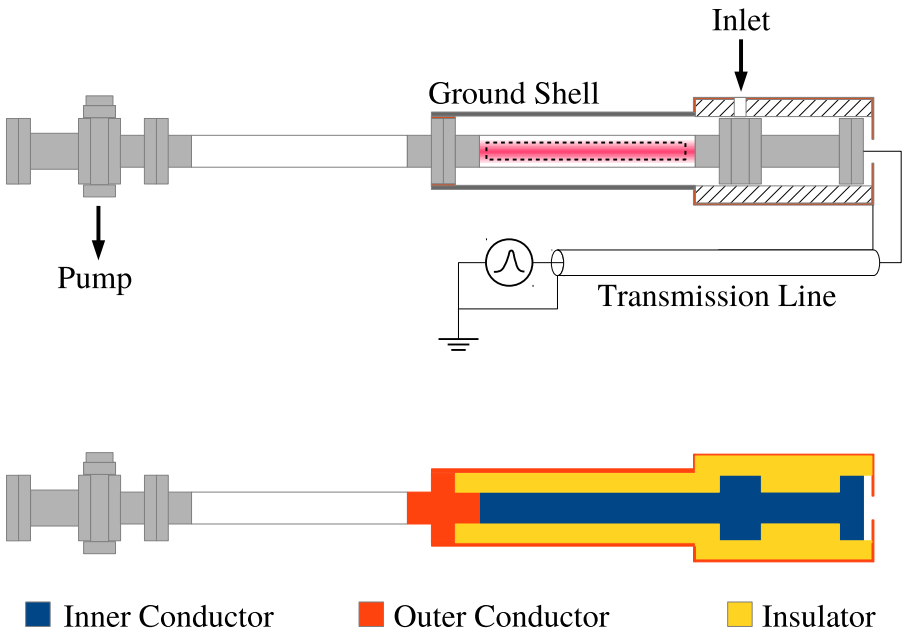

Figure 1.1: Two illustrations of the RPND apparatus. The upper version is an annotated sketch of the device, and the bottom version simplifies the geometry into its three electrical components.

The tube was composed of borosilicate glass with 2.75 in Conflat flanges on both ends. The plasma was generated inside the glass tube after it had been evacuated of air and filled with the desired pressure of helium. The tube had an inner diameter of 3.3 cm, an outer diameter of 4.0 cm, and a length of 22.9 cm. The overall length of the tube with the flanges was 30 cm. In the figure shown here, the right electrode served as the anode, and the left electrode was the cathode.

The dielectric surrounding the inner conductor was composed of several components. The vacuum window, nipple, double-sided flange, and anode were sep-

arated from the outer conductor by an air gap and a polytetrafluoroethylene (PTFE) tube (hatched in the figure), 20 cm in length with an inner diameter of about 7.5 cm, and an outer diameter of 10 cm. The plasma portion of the inner conductor was separated from the outer conductor by an air gap and the glass tube.

The cathode connected to the outer conductor and served as part of the current return path. Attached to the cathode was an aluminum tube (referred to as the ground shell), held in place by a acetyl resin shaft collar and copper shim.[1] Radial optical access to the discharge was provided by two slots milled into the ground shell. The slots were positioned on opposite sides of the shell and were 3.8 by 25.4 cm in length. The tube itself was 30 cm in length.

At the end nearest to the anode, the aluminum tube was affixed to a copper sheet, 10 cm square, with conductive copper tape. A 5 cm diameter hole was cut into the copper sheet to allow the discharge tube to pass through it. The sheet was secured to the PTFE tube by nylon screws. Surrounding the PTFE tube was a second shell, made of copper sheet. This was connected to the aluminum tube by a braided copper strap. The right end of the PTFE tube was covered by a second copper sheet, 10 cm square. The sheet was secured to the PTFE tube by nylon screws and in electrical contact with the copper shell. In the center of the copper sheet was a HN bulkhead adapter for connection to the transmission line. The inner conductor of the bulkhead adapter was connected by a straight run of 5 cm of silicone-coated wire to the vacuum window flange.

The voltage pulse was generated by a FID power supply, supplied by ANVS,

[1] While all of the aluminum tube is nominally at ground, it is likely that it would float to a finite voltage with each pulse.

Inc. (model PT510NM). The amplitude of each pulse was fixed at 6.4 kV with a repetition rate of 1.0 kHz. Each pulse had a fixed width of 25 ns, with a 10%-90% rise time of approximately 4 ns and was roughly Gaussian in shape. From a practical standpoint, the high impedance prior to breakdown should effectively double the peak voltage at the anode. A SRS DG645 delay generator was used to trigger the power supply output for all experiments and provided a reference time base for all measurements.

Preliminary experiments revealed multiple reflections between the power supply and the anode. A 13.7 m transmission line, made of RG213 coaxial cable, was used to isolate the reflections so that the effect of individual pulses could be examined. The calculated delay of the transmission line was 69.2 ns, for a total separation time between the pulse and the reflection of 138.4 ns. The calculated delay was found to be a close match in the measured delay.

The gas inlet connection was made through the double-sided flange via a 1/8" NPT hole. A 1/4" polyethylene tube was attached to the NPT connection via a NPT to 1/4" Swagelok adapater. The tube was then connected to a source of ultra-high purity (99.999%) helium. Throughout the experiment, the helium flow rate was fixed at 25.0 sccm with a digital flow controller, regardless of the operating pressure.

The discharge apparatus was pumped down by a oil-based roughing pump with an upstream zeolite trap. The pump was connected to the discharge tube by a second glass tube, intended to electrically isolate it from the cathode. The base pressure of the system was approximately 15 mTorr. The leak rate was measured

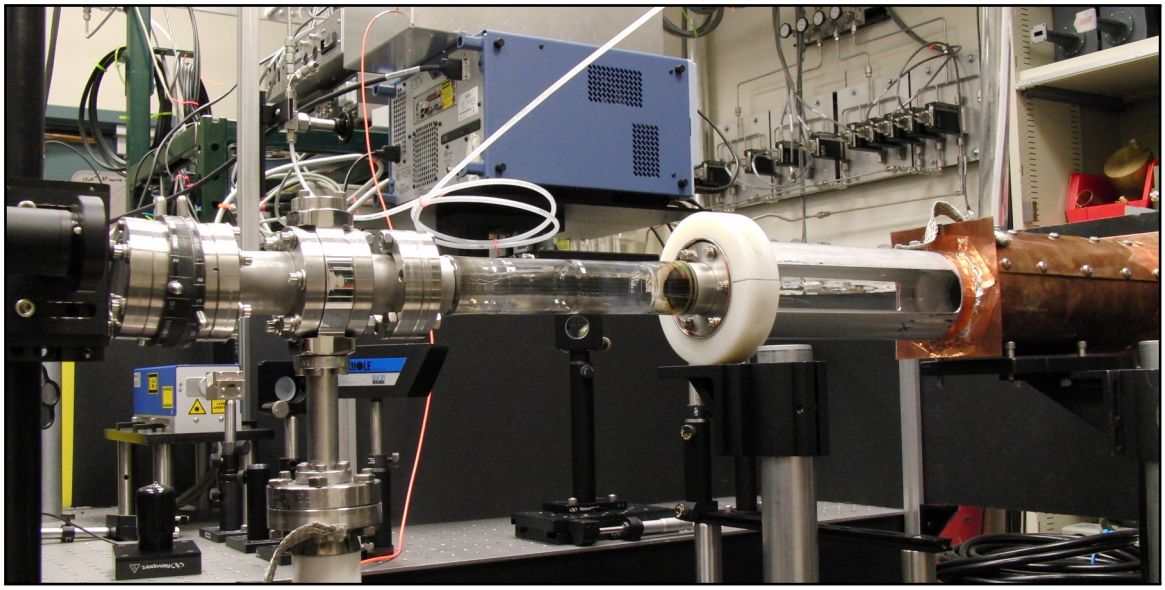

Figure 1.2: Photograph of the discharge apparatus.

several times by evacuating the apparatus and then sealing it from the pump with a bellows valve. The leak rate was found to be 2.0×10^{-3} sccm. Given a constant flow rate of 25.0 sccm, the fractional impurity can be conservatively estimated to be 80 ppm.

A MKS PDR-C-2C power supply and readout, and two capacitance manometers were used to measure the pressure. One manometer had a full scale range of 10 Torr, while the other had a range of 100 Torr. The desired pressure was obtained by sealing the system from the pump with the bellows valve. Two bypass pump lines, fitted with needle valves, were then used to adjust pumping speed and system pressure.

The assembled discharge apparatus can be seen in figure 1.2. The RPND apparatus was supported two 1.5 in mounting posts with angle brackets. The mounting

posts attached to a 4 ft by 2.5 ft optical breadboard, supported by urethane shock absorbers, and a rigid frame. The roughing pump was attached to the apparatus with flanged bellows in order to reduce vibrations.

All electrical measurements were made with a LeCroy 6100A WaveRunner oscilloscope which had a bandwidth of 1.0 GHz. Electrical connections to the oscilloscope were made with RG 50/U coaxial cable and standard BNC connectors, terminated at 50 Ω unless otherwise noted. The voltage of the pulses was monitored from $1:1000$ divider built into the power supply. The current was measured from a current shunt located in a break of the outer conductor of the transmission line. The current shunt was composed of 9, low inductance, 1.0Ω resistors connected in parallel. Figure 1.3

Data were retrieved from the oscilloscope with a desktop computer via the GPIB interface. Instrument control, data acquisition, and data storage were all managed by a LabView program. Analog input and output was handled with the auxiliary input and output ports of a SRS SR850 DSP lock-in amplifier.

1.2 Field Calculations

The electric field characteristics of the discharge system was analyzed using a two-dimensional, electrostatic solver, Ansoft Maxwell 9. Figure 1.4 is a heat map on a logarithmic scale, of the electric field magnitude, with overlaid electric field vectors (in magenta). The electric field varies significantly over the length of the discharge apparatus, with a peak near the axial location of the glass tube

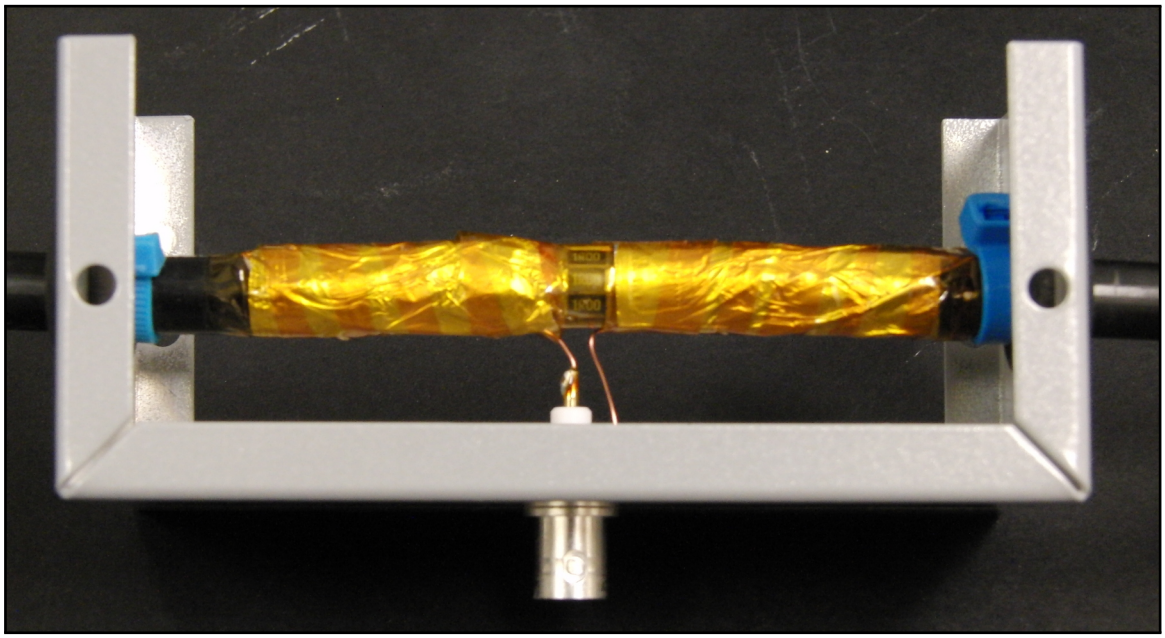

Figure 1.3: Photograph of the back-current shunt used to measure the current characteristics of the RPND.

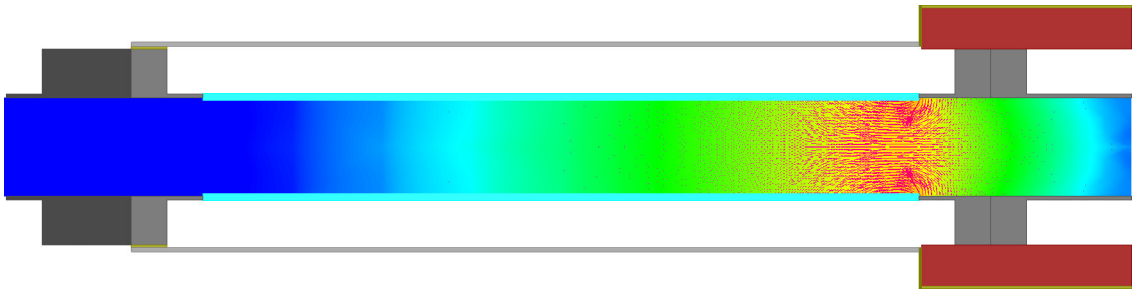

Figure 1.4: Heat map and vector plot of the electric field in the RPND discharge apparatus.

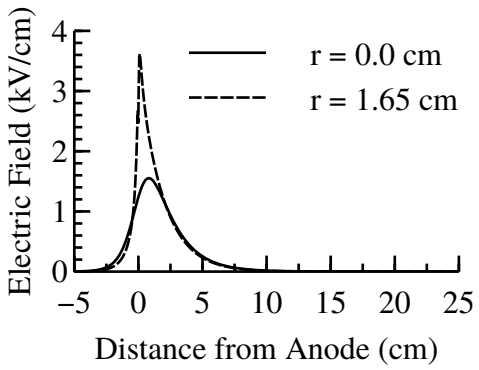

Figure 1.5: The magnitude of the electric field along the center and outside of the discharge apparatus.

followed by a monotonic decline. These characteristics are a large departure from simple case of two parallel electrodes in which the field is uniform throughout. This can be attributed to the presence of the external ground shield. Though this does complicate the field characteristics, the proximity of the ground results in a much higher electric field than would otherwise be achievable.

While the off-axis field lines all feature notable radial components, particularly close to the anode the center line does not. Figure 1.5 is a plot of the magnitude of the electric field along the central axis of the discharge apparatus and the outside, adjacent to the glass tube. The location of the anode is defined as the location of the glass-to-metal seal. The field close to the triple point at the seal is the highest at approximately 3.5 kV/cm, while the field along the axis peaks at about 1.5 kV/cm. At a distance of 2 cm from the anode, the electric field magnitude is roughly the same regardless of the radial coordinate. At the measurement locations of 3.83, 11.45, and 19.07 cm, the vacuum electric field

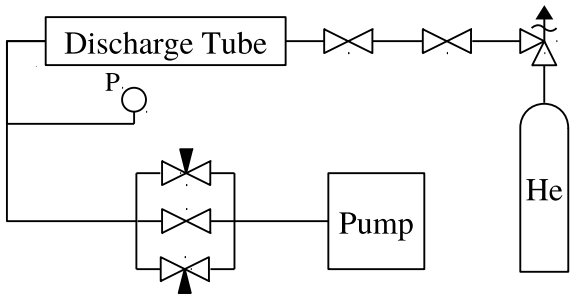

Figure 1.6: Simplified diagram of the gas flow path and pumping system.

was 4.8×10^5, 750, and 11 V/m respectively.

1.3 Operating Procedures

One of two operating procedures was selected depending on how recently the plasma had last been turned on. If it had been greater than one hour, a full startup procedure was used. Otherwise, an abbreviated process was used.

In order to obtain consistent discharge characteristics, it was necessary to develop two sets of operating procedures for the RPND. In the case that the discharge had not been operated for over an hour, the roughing pump was turned on and the primary pump path valve was opened as was the first shutoff valve upstream of the discharge chamber, seen in figure 1.6. The system was then allowed to pump down to its base pressure. Afterward the final shutoff valve upstream of the pump path was opened and the system was again allowed to reach base pressure. At this point the helium flow was turned on and set to 25.0 sccm. The primary pump path was then closed and the needle valve bypasses were used to adjust the system

pressure to 3.0 Torr.

Next, the delay generator was turned on and the output for triggering the power supply was activated. Then, the FID power supply was then turned on. This would produce an easily visible plasma within the discharge tube. The system was allowed to operate at this condition for one hour in order to remove potential contamination on the walls and electrodes. At the end of this period, the pulse voltage waveform was checked to ensure that it was consistent with previous waveforms. Once this was confirmed, the pressure was adjusted to the desired operating condition.

The plasma was shutdown by first shutting off the power supply, followed by the delay generator. Then, the helium flow was shut off, and the primary pump path was opened. The system was allowed to come to base pressure before the two upstream shutoff valves were closed, after which the primary pump path was closed. The roughing pump was then shut off.

In the cases that the plasma had been operated within the last hour, it was possible to use an abbreviated startup procedure. This process was fundamentally the same as the previous one, however the plasma only required five minutes to reach a steady state. This was verified with multiple measurements of the current and voltage characteristics as well as the plasma emissions. At times prior to this five minute equilibration period, the reflected pulse energy was noticeably higher, and the delay between the trigger pulse and the output pulse was variable.

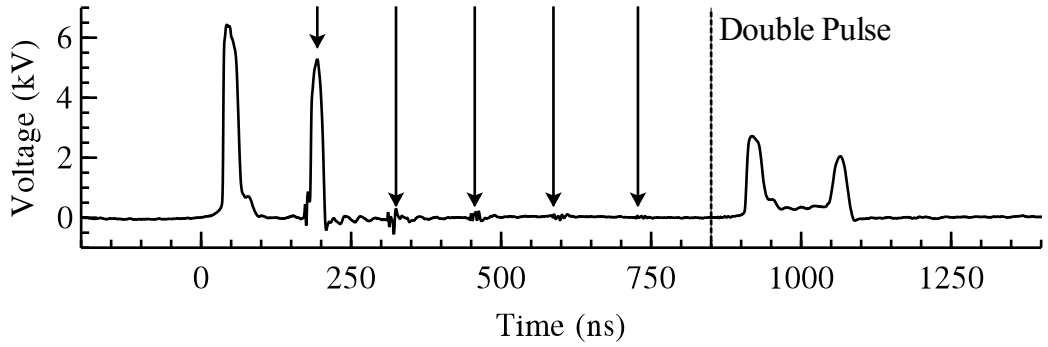

Figure 1.7: Typical voltage waveform of the RPND. Arrows indicate reflections back to the power supply. The dotted line delineates the time at which the power supply begins to exhibit double pulsing.

1.4 Electrical Characteristics

The general voltage waveform of the RPND showed a number of characteristics. Figure 1.7 is a plot of a typical voltage waveform of the RPND. It begins with an incident pulse with a small foot at $t = 0.0$. This followed by a reflected pulse 138 ns afterward. The reflected pulse is somewhat attenuated, proportional to the energy deposited in the plasma. Additional reflections are visible at integer multiples of 138 ns, however they are highly attenuated. This suggests that after the first pulse initiates the discharge, energy is much more easily coupled into the volume. An additional pulse appears after about 800 ns. This is believed to be a peculiarity of the power supply. For the most part, analysis of the RPND will focus on the first 138 ns in order to isolate the effects of a single pulse.

The independent variable for most operating conditions was the pressure of the system. The properties of the RPND were examined at: 0.3, 0.5, 1.0, 2.0, 3.0,

4.0, 8.0, and 16.0 Torr. The appearance of the plasma varied with the pressure in a continuous fashion, however it was apparent that there were three regimes of operation.

At the low pressures, 0.3 and 0.5, it was difficult to initiate the discharge. Often, it would be necessary to increase the pressure to initiate the discharge, and then reduce the pressure to the desired conditions. The plasma appeared dim and relatively constricted to the central axis of the discharge tube, with a radial extent of approximately 1 cm. Accompanying these presures was a large degree of electronic noise. This manifested in the voltage and current waveforms, seen in figure 1.8, as well as a number of equipment malfunctions.

As the pressure was increased (from 1.0-4.0 Torr), the electrical noise began to subside. The waveforms in figure 1.8 show significant reductions in the ringing that was particularly prominent in the current waveforms. In addition, the visual extent of the plasma increased substantially to the point where it could be considered volume-filling. The plasma also increased its axial extent as well, eventually reaching well past the cathode/ground. This was despite attempts to isolate this portion of the apparatus from the plasma. It is possible to attribute this to the relatively large surface area of the anode in comparison to the cathode. If a sufficiently high electron current is being drawn from the cathode, space charge could begin to limit further current extraction.

However, the plasma receded back to the intended cathode structure at the higher operating pressures, 8.0 and 16.0 Torr. This was accompanied by a decrease in the apparent brightness of the plasma to levels similar to that of the low

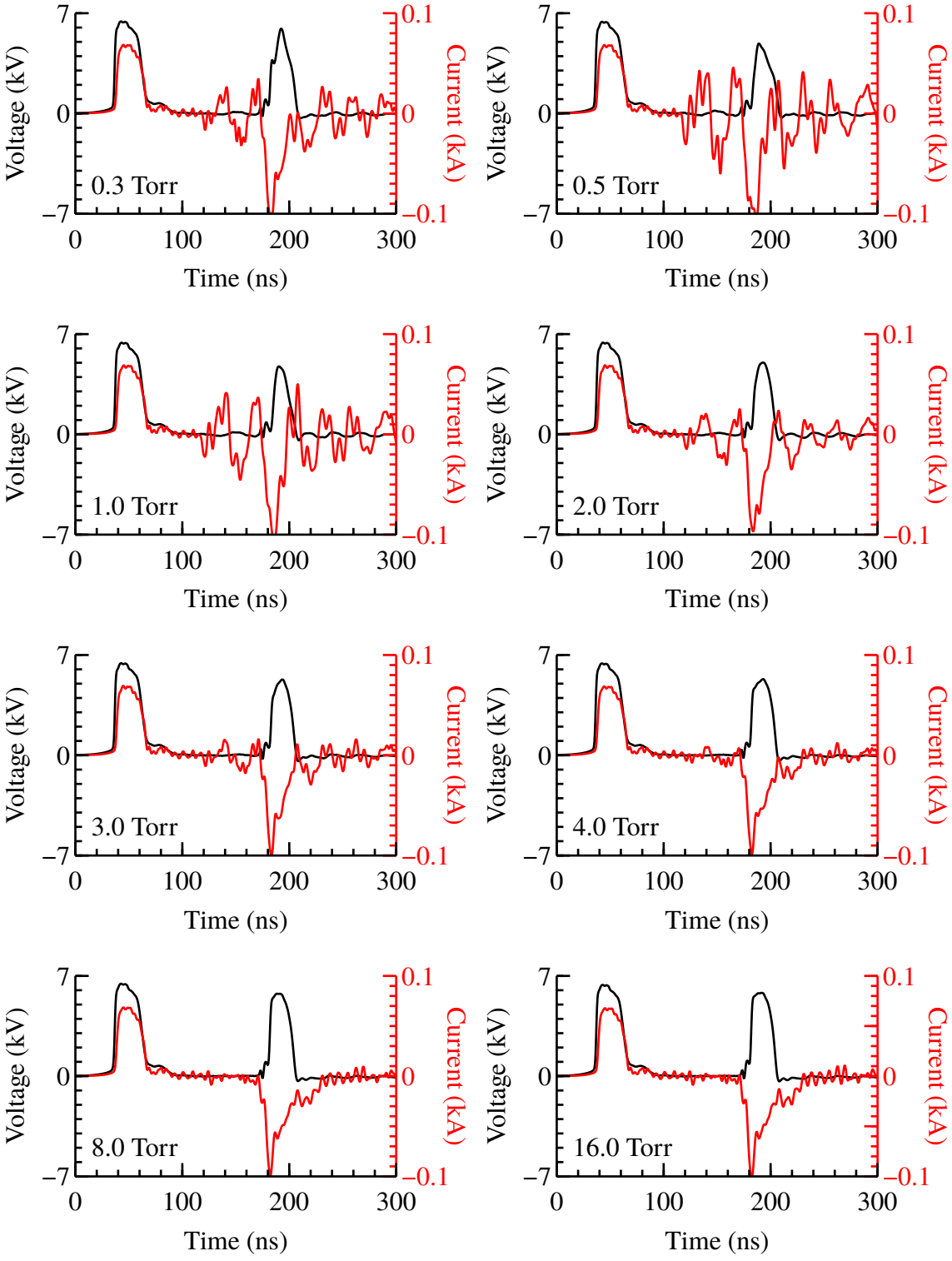

Figure 1.8: High resolution views of the voltage and current waveforms for the first incident and reflected pulse, at each of the operating pressures.

pressure conditions. In contrast, the plasma appeared to remain volume-filling. While discharge initiation was difficult at the higher pressures, it was not accompanied by the electrical noise observed at lower pressures.

1.5 Energy Coupling

The product of the voltage and current waveforms as seen in figure 1.8 gives the power deposited in the plasma as a function of time. Subsequently, the power integrated over time gives the total energy deposited in the plasma. However, this approach is somewhat complicated several features of the RPND. As previously mentioned, the pulses produced by the power supply are not completely absorbed by the plasma. Therefore, the integration must be carried out over both the incident and the reflected pulse. Additionally, there is the concern that the oscillations in the current measurements could introduce fluctuations in the calculated energy deposition. However, the small voltage signal limits the error introduced by these fluctuations to less than 1%.

Figure 1.9 gives the total energy deposited for the first pulse at each of the operating conditions. The energy coupled to the plasma peaks at an energy of 5.5 mJ at a pressure of 1.0 Torr, after which it slowly decreases. This peak in the coupled energy is coincident with the peak brightness of the plasma. Together, these suggest that the density of excited states will be optimized at intermediate pressures.

Though there appear to be no direct comparisons available in the literature,

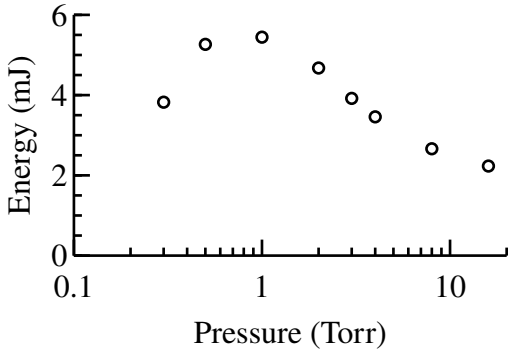

Figure 1.9: Plot of the energy coupled into the plasma with the first pulse as a function of pressure.

several papers report on energy coupling for similar systems. Macheret, Schneider, and Murray studied a parallel plate RPND in air, at 1-10 Torr and reported a total energy deposition of 0.30-0.36 mJ, increasing with pressure [2]. Nishihara et al. recorded values of 1-2 mJ in a nitrogen RPND [3]. Pancheshnyi et al., in the study of an air-propane mixture at 750 Torr, found that each pulse deposited about 1.9 mJ of energy.

From an applications standpoint, potential existence of a condition which optimizes the production of excited states is an interesting one. From a physical standpoint, the growth and decline of energy deposition is with power is compelling as it suggests two or more competing processes. Though this kind of competition is reminiscent of Paschen's law, the duration of the pulse is too short for appreciable ion drift (about 3 mm for the maximum field from the electrostatic simulations), therefore secondary electron emission is not important. These observations provide additional impetus for a closer examination of the RPND prop-

erties, particularly the excited states.

Bibliography

[1] L M Vasilyak, S V Kostyuchenko, N N Kudryavtsev, and I V Filyugin. Fast ionisation waves under electrical breakdown conditions. *Physics-Uspekhi*, 37(3):247–268, March 1994.

[2] S. O. Macheret, M. N. Shneider, and R. C. Murray. Ionization in strong electric fields and dynamics of nanosecond-pulse plasmas. *Physics of Plasmas*, 13(2):023502, 2006.

[3] Munetake Nishihara, J. William Rich, Walter R Lempert, Igor V. Adamovich, and Sivaram Gogineni. Low-temperature M=3 flow deceleration by Lorentz force. *Physics of Fluids*, 18(8):086101, 2006.